Nuclear Instruments and Methods in Physics Research B 549 (2024) 165288

Contents lists available at ScienceDirect

Nuclear Inst. and Methods in Physics Research, B

journal homepage: www.elsevier.com/locate/nimb

Full Length Article

Investigation of the synergistic effects on 4H-SiC junction barrier Schottky Diodes after multiple irradiation

Mu He [a], Xiaoping Dong [a], Meiju Xiang [a], Yao Ma [a,b,*], Mingmin Huang [a,b], Sijie Zhang [a,b], Qingkui Yu [c], Shuang Cao [c], Zhongyu Lu [d], Yun Li [a], Zhimei Yang [a,b], Min Gong [a,b]

[a] Key Laboratory of Microelectronics, College of Physics, Sichuan University, Chengdu, 610065, China
[b] Laboratory of Radiation Physics and Technology of Ministry of Education, Sichuan University, Chengdu 610065, China
[c] China Academy of Space Technology, Beijing 100029, China
[d] Dazhou Ten Pao lnnovation Technology Co., Ltd, Dazhou 635100, China

ARTICLE INFO

Keywords:
SiC JBS
Multiple irradiation
Deep level defects
Carrier mobility

ABSTRACT

In this work, the irradiation effects of 1200 V commercial silicon carbon (SiC) Junction Barrier Schottky Diodes (JBSs) were thoroughly studied at multiple irradiation conditions by choosing the typical energy and flux of heavy ions (HIs) and electrons. The electrical properties were measured and the relevant electrical parameters were extracted. It was demonstrated that heavy ion irradiation induced negligible deterioration since the total fluence was insufficient. Moreover, the electron irradiation had a significant impact on the conduction resistance forward conduction characteristics. Multiple irradiation results showed that the damage of devices under test (DUTs) mainly depends on the fluence of electrons rather than HIs. More specifically, deep-level transient spectroscopy (DLTS) was conducted to qualitatively explain the possible impact of the composite centers on mobility (μ_n) and carrier lifetime. In addition, the μ_n in the drift region of the different irradiated devices was quantitatively analyzed by performing TCAD simulations, and the relationship between mobility and irradiation fluence was obtained.

1. Introduction

It has been proved that silicon carbon (SiC) has excellent performance in spacecraft electronics due to its electrical and thermal properties [1,2]. Recently, SiC-based power electronic components are currently offering sustainable solutions to replace conventional silicon (Si) devices in harsh environment applications, which can significantly reduce the total weight of the spacecraft. 4H-SiC Junction Barrier Schottky Diodes (JBSs) are currently widely used in aerospace applications, electric vehicles, solar inverters, industrial power supplies, and so on. In aerospace, electric facilities work in a compound environment with various irradiation sources and wide temperature ranges, challenging the irradiation resistance and reliability of both circuits and devices.

For instance, the irradiation effects of different sources, such as protons, electrons, and heavy ions (HIs) on 4H-SiC JBSs have been thoroughly studied [3–5]. However, the ground simulation irradiation experiments only target a single irradiation source. Electronic devices in space are irradiated by multiple kinds of particles, making them more sophisticated for real irradiation damages. In order to better restore the space irradiation environment, the distribution of heavy ions and electrons was considered here.

The space irradiation environment mainly comes from the geomagnetic field capture zone (also known as the Van Allen Belt), solar cosmic rays, and galactic cosmic rays [6–9]. The energy range of heavy ions is very wide in the geomagnetic field capture zone, ranging from tens of MeV to several GeV, with high linear energy transfer (LET). Although the average flux of HIs in space is relatively low (taking the particles studied in this paper as an example, the flux is around 1E-8 ions/(cm^2s) for LET = 37.4 MeV·cm^2/mg), their high LET values and the interactions with other particles (such as nuclear collisions, ionization, etc.) can have a significant impact on spacecraft. Compared to HIs, high-energy irradiative electrons in space have lower energy (ranging from a few keV to tens of MeV) and much higher flux. In the Van Allen belt, the flux of the 2 MeV-electrons is around 10 to 1E6 e/(cm^2s), which is 9 to 14 times the flux of HIs.

Therefore, in this work, the synergistic effects of heavy ion and electron irradiation on 4H-SiC JBSs were systematically studied. To this

* Corresponding author at: Key Laboratory of Microelectronics, College of Physics, Sichuan University, Chengdu, 610065, China (Yao Ma).
E-mail address: mayao@scu.edu.cn (Y. Ma).

https://doi.org/10.1016/j.nimb.2024.165288
Received 18 September 2023; Received in revised form 19 January 2024; Accepted 8 February 2024
Available online 15 February 2024
0168-583X/

Table 1
Details of the various irradiation conditions.

Irradiation sources	Fluences (e/cm^2 or ions/cm^2)	Flux (fluence/s)
205 MeV Ge ions	1E6	1.4E3
LET = 37.4 MeV·cm^2/mg	1E7	9.68E4
	1E8	1.03E5
1.7 MeV electron	1E14	1E13
	1E15	
	1E16	
Multiple irradiation	Ge ion fluences	Electron fluences
	1E6 ~ 1E8	1E15/1E16

*Multiple irradiation mean the DUTs were irradiated by 205 MeV Ge ion first, and then were placed under the 1.7 MeV electron beam.

Table 2
The names of the DUTs under multiple irradiation for short in this paper.

Multiple irradiation		HI irradiation		
		1E6 ions/cm^2	1E7 ions/cm^2	1E8 ions/cm^2
Electron irradiation	1E15 e/cm^2	M1	M2	M3
	1E16 e/cm^2	M4	M5	M6

end, irradiation experiments were conducted by choosing the typical energy and flux of HIs and electrons. After the irradiation, several testing and simulation works were carried out. The acquired data revealed that in this case, the irradiation damages were mainly caused by the induced electrons as the differences in total fluences between HI and electron irradiation.

2. Experimental

Commercial 4H-SiC JBSs (Infineon, IDW40G120C5B, 1200 V/40 A) were irradiated by both heavy ion and electron irradiation conditions. The heavy ion irradiation test was conducted at the HI-13 tandem accelerator, at China Institute of Atomic Energy (CIAE), producing a 205 MeV Ge ion beam. The LET was 37.4 MeV·cm^2/mg. On top of that, the electron irradiation test was conducted at the GJ-2 electron accelerator, at Sichuan Institution of Atomic Energy (SIAE). All the irradiation tests were conducted at room temperature (RT). The irradiation details and the names of devices under test (DUTs) for short are presented in Table 1 and Table 2, respectively. All the encapsulant materials of the DUTs were removed by laser decapsulation to make the active region exposed.

After the irradiation, the DUTs were electrically characterized with Agilent B1505A for capturing the high frequency (HF, 1 MHz) capacitance to voltage (*C-V*), breakdown characteristics, and Keysight B2902 for the forward current to voltage (*I-V*) characteristics measurements. Deep-level transient spectroscopy (DLTS) measurements were performed using Phystech FT1030 HERA-DLTS and a Genius CCS450 heating stage for temperature control. The reverse bias (U_R) and pulse voltage (U_P) were −8 V and 0 V, respectively. Furthermore, the period width (T_W) and pulse width (t_P) were 100 ms and 100 μs, respectively. The active areas of JBSs were estimated to be 2.43 mm^2 through the transmission electron microscopy (TEM) results of the device.

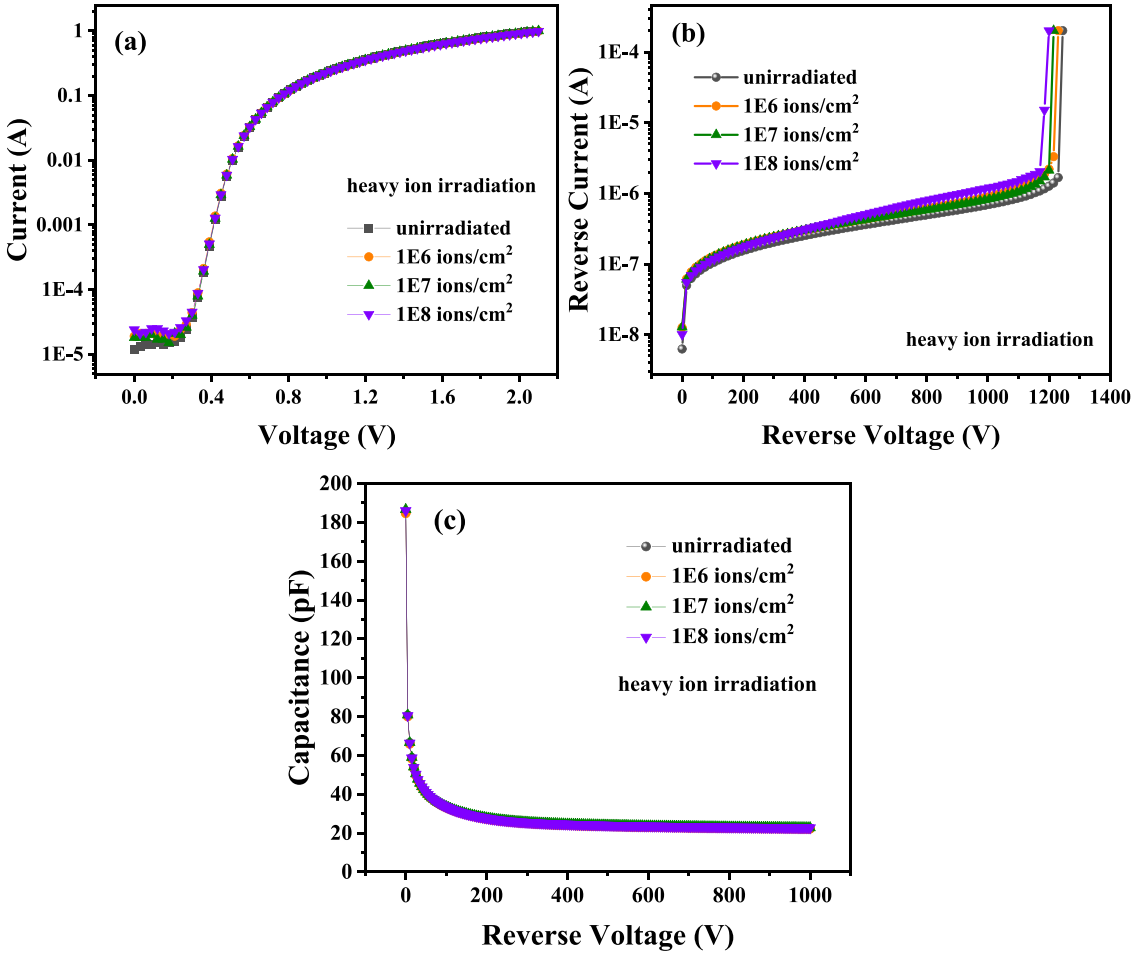

Fig. 1. The electrical characteristics of DUTs after HI irradiation: (a) semi-log forward *I-V*, (b) breakdown characteristics, and (c) *C-V* characteristics.

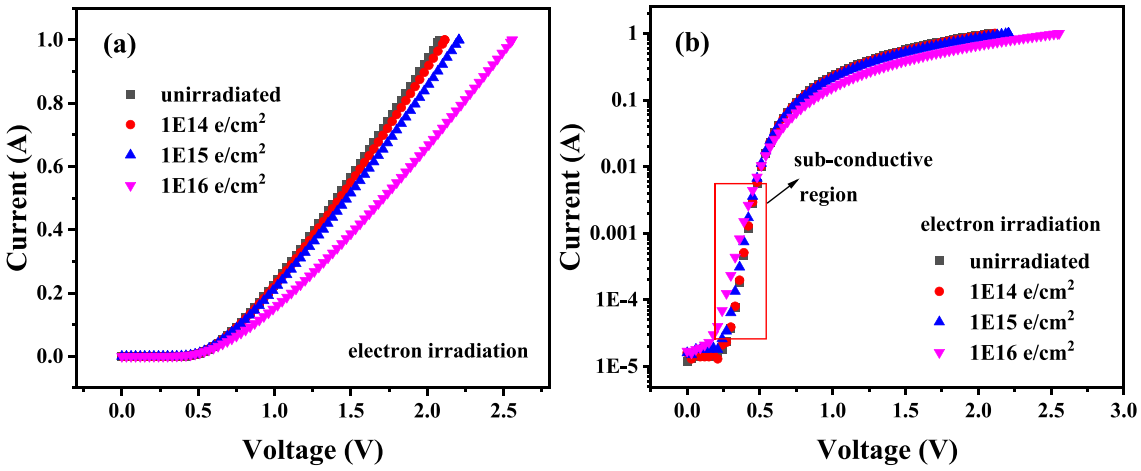

Fig. 2. The (a) linear and (b) semi-log forward *I-V* characteristics of DUTs after electron irradiation.

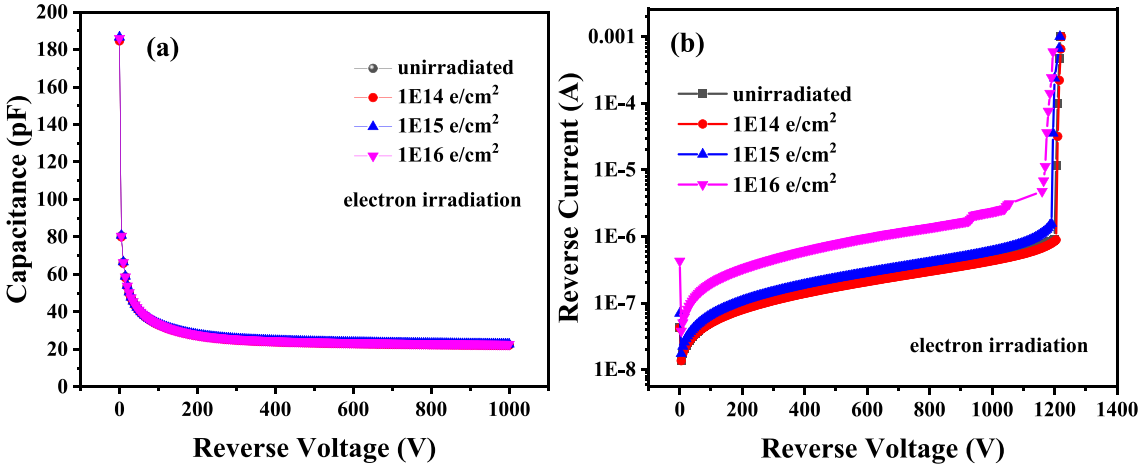

Fig. 3. The (a) *C-V* and (b) breakdown characteristics of DUTs after electron irradiation.

3. Results and discussion

3.1. Electrical characteristics

To investigate the impact of heavy ion and electron irradiation on the electrical properties of SiC JBSs, the *I-V* and *C-V* characteristics of DUTs were measured at RT. The electrical characteristics of SiC JBSs suffered from HI irradiation are shown in Fig. 1. It is obvious that the device characteristics have hardly deteriorated after simple HI irradiation. It can be assumed that the irradiation only caused damage to a small number of cells and did not significantly affect the electrical characteristics of the DUTs due to the low total fluences of HIs.

The forward conduction characteristics of the devices after carrying out simple electron irradiation are shown in Fig. 2. Obviously, after electron irradiation, the slope of the linear part of the *I-V* decreased in Fig. 2 (a), which indicates an increase in the conduction resistance. As can be seen in Fig. 2 (b), the slope of the sub-conductive region evidently decreased after 1E16 e/cm^2, which infers an increase in the ideality factor (n).

As shown in Fig. 3 (a), the capacitance properties remained unchanged compared to the unirradiated sample, indicating the small variation in the effective doping concentration (N_D, which is also called effective carrier concentration). In Fig. 3 (b) the breakdown voltage (BV) maintained around 1200 V, and only the sample irradiated at maximum fluences exhibited an apparent increase in the leakage current.

Based on the thermionic emission theory, several electrical parameters of power JBSs like ideality factor (n), series resistance (R_S), and zero-bias Schottky barrier height ($SBH_{I\text{-}V}$) can be extracted from the relationship between forward current (I_F) and on-state voltage drop (V_F) in Eq. (1) [10].

$$I_F = AA^*T^2 exp\left(-\frac{qSBH_{I-V}}{k_0T}\right) exp\left[\frac{q(V_F - I_F R_S)}{nk_0T} - 1\right] \quad (1)$$

where q is the elementary charge, k_0 is the Boltzmann constant, T refers to the absolute temperature, A represents the active area, and A^* denotes the Richardson constant (146 A·cm^{-2}·K^{-2} for 4H-SiC).

Additionally, the effective doping concentration N_D, flat-band Schottky barrier height ($SBH_{C\text{-}V}$) can be obtained from Eqs. (2) to (3) [11].

$$\frac{1}{C^2} = \frac{2}{qA^2N_D\varepsilon_s\varepsilon_0}\left(\Phi_{bi} - V - \frac{k_0T}{q}\right) \quad (2)$$

$$\Phi_{bi} = SBH_{C-V} - \frac{k_0T}{q}\left[\ln\left(\frac{N_C}{N_D}\right) + 1\right] \quad (3)$$

where ε_s is the relative dielectric constant of the semiconductor (9.7 for 4H-SiC), ε_0 stands for the vacuum permittivity, Φ_{bi} is the built-in potential, and N_C states the effective density of states of the conduction band (1.7E19 cm^{-3} for 4H-SiC).

The electrical parameters extracted by the static electrical characteristics of simple electron-irradiated samples are listed in Table 3. The

Table 3
The electrical parameters extracted from the *I-V* and *C-V* characteristics after electron irradiation.

Samples	unirradiated	1E14	1E15	1E16
R_s (Ω)	1.37	1.40	1.50	1.79
n	1.03	1.09	1.18	1.72
$SBH_{I\text{-}V}$ (eV)	1.17	1.15	1.08	0.96
N_D (cm^{-3})	8.53E15	8.55E15	8.68E15	8.76E15
$SBH_{C\text{-}V}$ (eV)	1.69	1.69	1.71	1.74

degree of deterioration of R_s, n, and $SBH_{I\text{-}V}$ was positively correlated with the total electron fluences. Among them, the changes in R_s and n were particularly significant. The conduction formula has been shown in Eq. (1), wherein the forward voltage drop V_F can be expressed as Eq. (4).

$$V_F = V_{FS} + V_R = V_{FS} + V_D + V_{SUB} + V_{CONT} \tag{4}$$

where V_{FS} is the forward voltage drop across the Schottky contact, V_R denotes the resistive voltage drop including V_D, V_{SUB}, and V_{CONT}, which represent the voltage drop across the drift region, substrate, and the ohmic contact to the cathode, respectively.

As irradiation has a negligible impact on substrate resistance and ohmic contact resistance, the increase of R_s may be due to the resistance of drift region R_D. It is considered that there is probably no variation in the values of N_D in the samples after irradiation, since the slight changes fall within the margin of device uniformity error. Therefore, the possible reason for the increase of R_D is the decrease in carrier mobility (μ_n). The ideality factor n is an indicator of the type of current conduction mechanism inside the Schottky junction, exhibiting the same trend as R_s. When n is close to 1, it indicates that the tunneling current or depletion layer composite is small or absent, the saturation current is determined by thermal electron emission. Consequently, the significant increase in the ideality factor indicated that the current conduction mechanism at 1E16 e/cm^2 had seriously deviated from the thermal electron emission theory. Besides, the incident particles can cause the inhomogeneity of the barrier's height [12]. The decrease of $SBH_{I\text{-}V}$ will cause an increase in the tunneling current, and the defects induced by irradiation play a role in recombination centers, which lead to an increase in the recombination current.

The N_D calculated by high-voltage *C-V* was almost no change after electron irradiation, which is different from the previous results of carrier removal effects [13–16]. The difference may by caused by: (1) the differences between the fabrication process for the samples in this manuscript and samples in the previous work; (2) the carrier removal rate η in previous studies may be not accurate enough due to using the low-voltage *C-V* data.

In order to explain the values of N_D obtained through low-voltage *C-V* data are not accurate, TCAD simulation was used to study the depletion region thickness (W_{dep}) and N_D corresponding to various reverse biases in *C-V* tests. A pure Schottky junction (parallel planar junction)

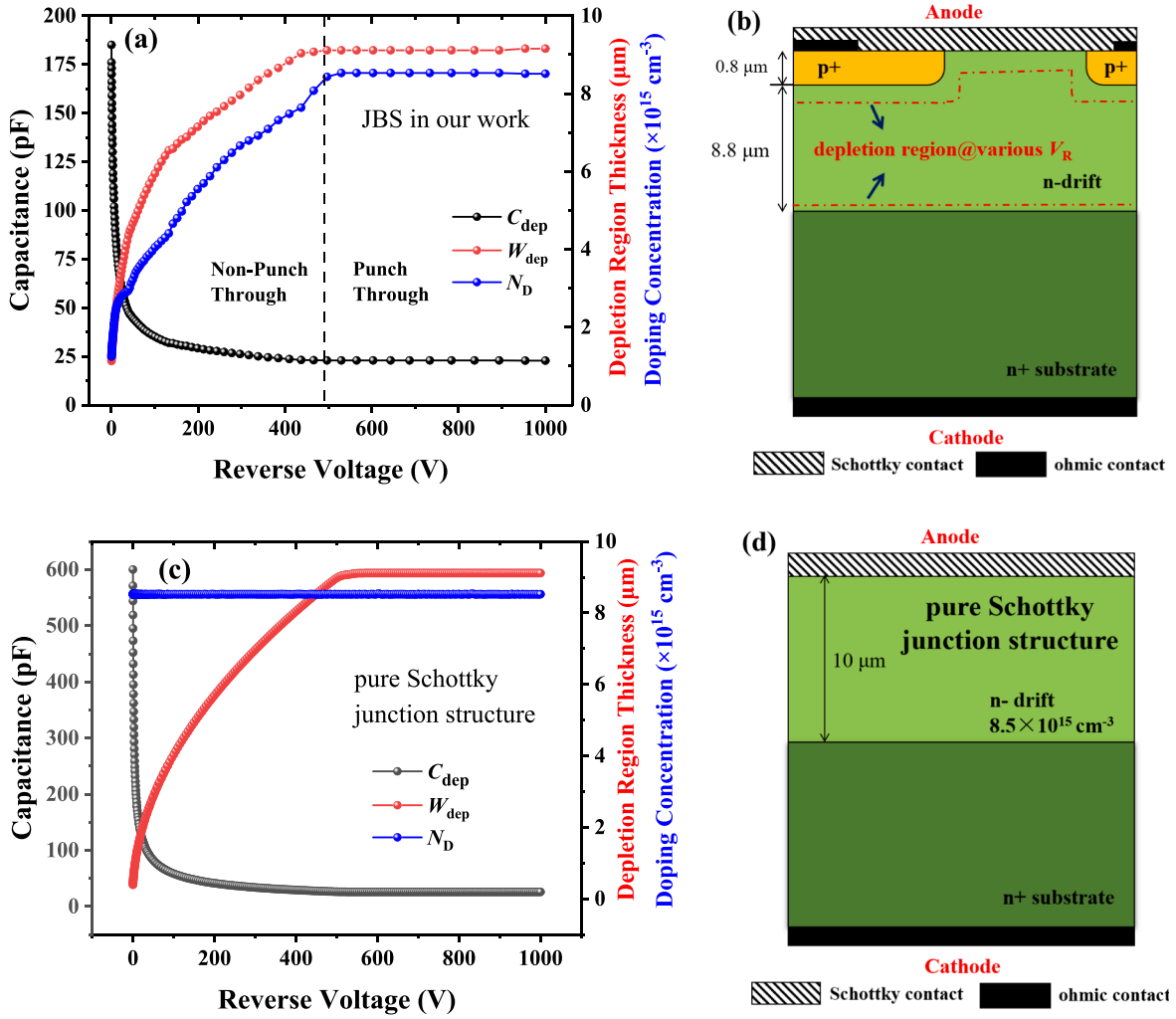

Fig. 4. Comparison of (a) JBS and (c) pure Schottky junction structure on *C-V* and values of W_{dep} and N_D under given values of reverse bias, (b) and (d) are the schematic diagrams of the two structures.

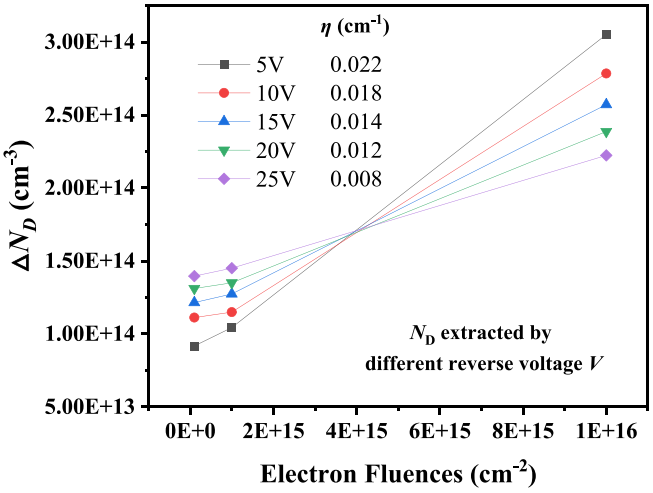

Fig. 5. The carrier removal rate η calculated at different reverse voltage from low-voltage *C-V* results.

structure with the same N_D value (8.5E15 cm^{-3}) is also used as a comparison, as shown in Fig. 4. It can be found from Fig. 4 that the value of N_D extracted at low voltage is accurate for the case of the pure Schottky junction, since the pure Schottky junction case is an ideal parallel planar capacitor. However, the accurate value of N_D should be obtained under a punch through voltage (the n-drift is fully depleted) for the case of the JBS. As for the JBS diode, under low voltage conditions, the junction capacitance of devices is not an ideal parallel planar capacitor (most equipotential lines are curved, not parallel, and the built-in potentials of PN junction and Schottky junction are uneven), leading to inaccurate N_D calculations and inaccurate carrier removal rate η.

Fig. 5 shows the value of η calculated by the tested low-voltage *C-V* data. It can be seen that inaccurate N_D will lead to inaccurate carrier removal rate η, where the value of η increases as the reverse bias voltage used for calculation decreases. However, no carrier removal effect can be found by using the tested high-voltage *C-V* data.

In addition, the electrical characteristics of SiC JBSs suffered from multiple irradiation are shown in Fig. 6. All the *C-V* characteristics after various irradiation conditions were kept unchanged, similar to Fig. 1 (c). In multiple irradiation, the damage of DUTs mainly depends on the fluence of electrons rather than HIs, as can be seen in Fig. 6, indicating that the fluence of HIs is still insufficient to cause significant damage to the sensitive area of the devices though the energy and LET are quite high.

3.2. DLTS results

Defects induced by irradiation have been widely researched in SiC Schottky barrier diodes (SBDs) and JBSs [17–19]. Deep level impurities generally have low concentrations, and their impact on the carrier concentration and conductivity type in semiconductors is not significant compared to shallow level impurities [20]. However, their recombination effect on carriers is stronger than that of shallow level impurities, so deep level impurities are also known as recombination centers, mainly impacting the carrier lifetime (τ) and mobility (μ_n).

In order to explore the possible reasons for the changes in carrier mobility, defect characterization of the samples was carried out by conducting DLTS tests [21]. The DLTS results after various irradiation conditions are shown in Fig. 7. As the normalized DLTS signal amplitude is nearly proportional to the defect concentration (N_T), it can be seen that the N_T of induced defects after electron irradiation is much greater than that induced by HI irradiation, related to the irradiation fluences. This can also confirm the varying degrees of degradation in the electrical characteristics of DUTs under different irradiation conditions.

For the Schottky diode, the choice of the U_R and U_P determines the detection range of the transient signals. The spectrum information comes from the M−S interface when the value of the pulse voltage is close to 0. On the contrary, when the value is bigger, defect information from the body-SiC region can be derived. The energy level (E_C - E_T) and the capture cross section (σ_n) of the defects can be extracted by Eq. (5).

$$\ln(\tau_e v_{th} N_C) = \frac{E_C - E_T}{kT} - \ln(X_n \sigma_n) \tag{5}$$

where v_{th} is the thermal velocity of electrons, N_C refers to the state density of the conduction band, and X_n stands for the entropy factor. By using the linear regression method, the slope E_C - E_T and the intersection $\sigma_n X_n$ can be obtained. Moreover, the capture cross section reflects the defects' coulomb interaction with carriers. The extracted electronic properties of defects are presented in Table 4.

Fig. 7(a) displays that three defect peaks are formed after simple HI irradiation, labelled as P1, P2, and P3, where P1 (E_V + 0.34 eV) is the donor defect, and P2 (E_C − 1.06 eV), and P3 (E_C − 1.17 eV) are the acceptor defects. The P1 trap is associated with carbon split interstitials close to the silicon site $(CSi)_{Si}$ or carbon site $(CC)_C$ [22]. P2 and P3 are both deep level traps related to EH5, which is thermally stable. The possible physical origin of EH5 is carbon vacancies V_C or carbon interstitials C_i [23]. It has been clarified that C_i contribute more to the carrier mobility degradation compared to the carbon antisites C_{Si}, silicon antisites Si_C, and other type of defects [24]. Since the N_T of defects induced by HI irradiation are quite low compared to the doping concentration N_D, where all the N_T are no more than 1E13 cm^{-3}, the

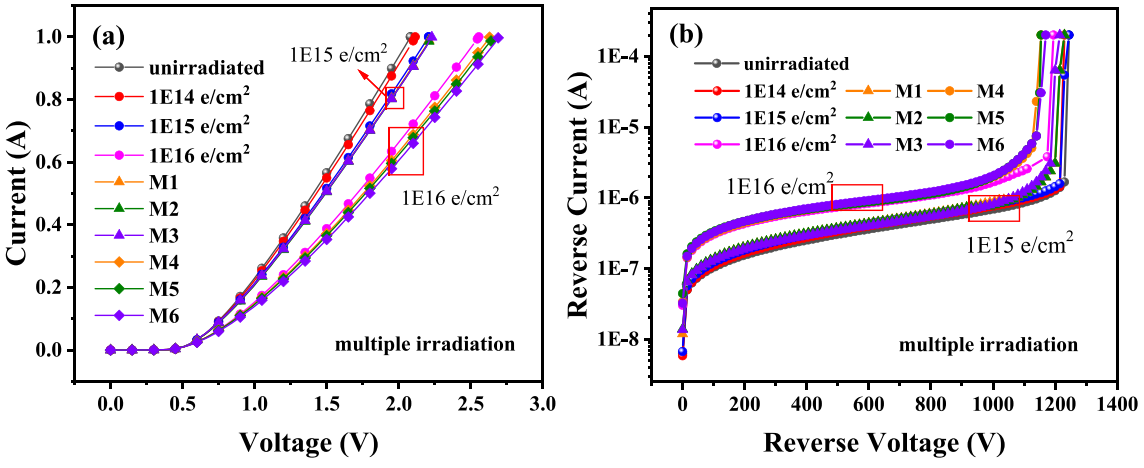

Fig. 6. (a) Forward *I-V* and (b) breakdown characteristics of the samples exposed to multiple irradiation.

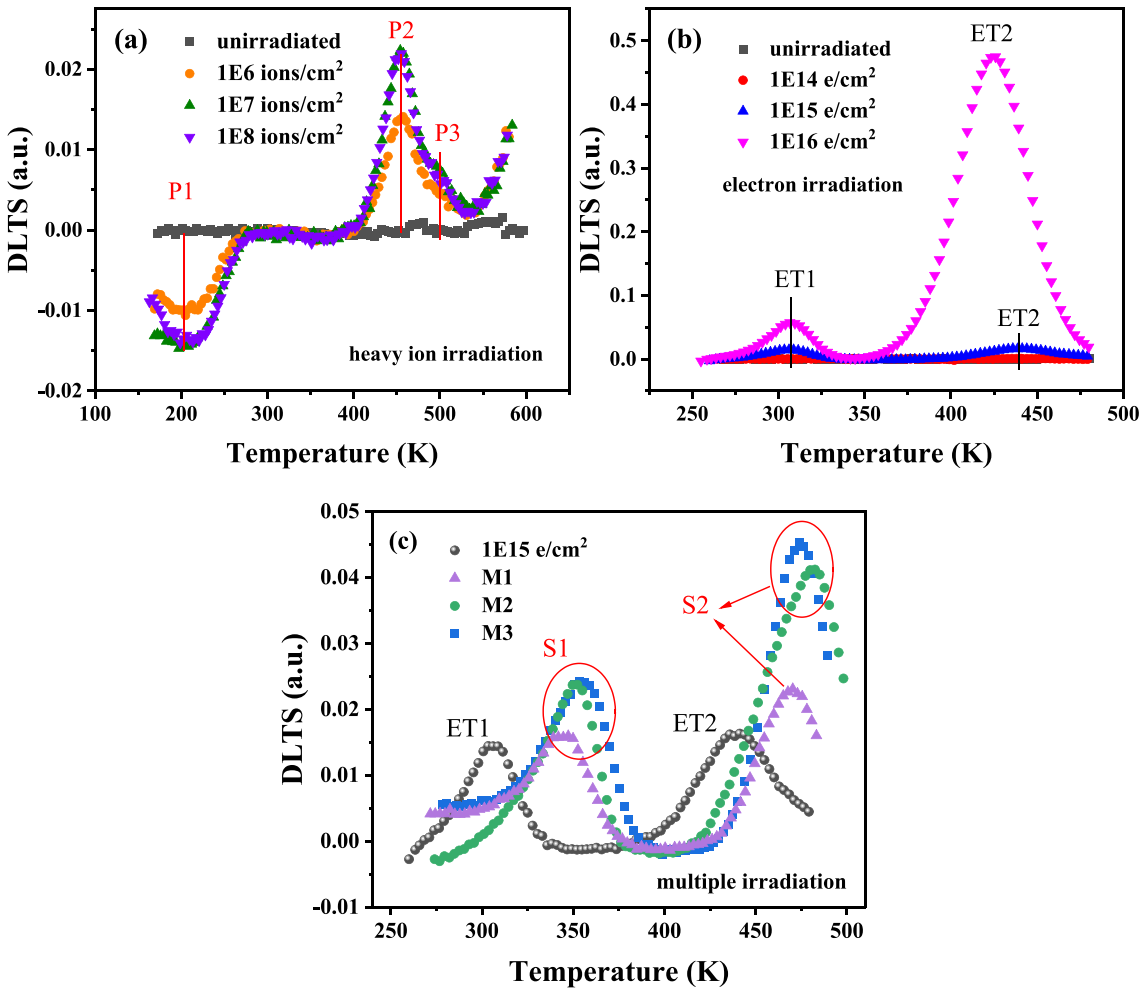

Fig. 7. Normalized DLTS results after (a) HI irradiation, (b) electron irradiation, and (c) multiple irradiation under different fluences.

Table 4
The electronic properties of the deep level defects detected by DLTS after different irradiations.

Sources	Labels	Peak temperature (K)	Energy level (eV)	Defects
HI irradiation	P1	210	0.34	C_i
	P2	455	1.06	EH5
	P3	495	1.17	
Electron irradiation	ET1	308	0.68	Z_1/Z_2
	ET2	440@1E15	1.01	$RD_{1/2}$
		427@1E16	0.96	
Multiple irradiation	S1	350	0.80	Fusion of multiple levels
	S2	480	1.07	$RD_{1/2}$/EH5

additional impurity scattering induced by HI irradiation is not very obvious.

Fig. 7(b) shows that the defects caused by simple electron irradiation are totally different. No defect peaks were detected in both the unirradiated and 1E14 e/cm^2 samples. Additionally, two independent peaks were found in 1E15 and 1E16 e/cm^2 samples labelled as ET1 (E_C − 0.68 eV) and ET2 (E_C − 0.96 ~ 1.01 eV). ET1 is related to carbon vacancies V_C attributed to the Z_1/Z_2 center [25,26], and is widely detected in implanted materials and the electron irradiated materials as an intrinsic defect, which destructively affects the carrier lifetime [27,28]. ET2 is associated with acceptor-like trap $RD_{1/2}$, which is one carbon vacancy and one silicon vacancy ($V_C + V_{Si}$) located on the adjacent lattice site [29]. Both deep-level defects mainly affect carrier lifetime rather than doping concentration.

The new defect peaks in M1 ~ M3 at around 350 K and 480 K appeared to be generated by the combined action of electron and HI irradiation in Fig. 7(c), labelled as S1 (E_C − 0.80 eV) and S2 (E_C − 1.07 eV), respectively. The comparison results of M4 ~ M6 and 1E16 e/cm^2 samples were similar to Fig. 7(c). S1 has been found in Ref. [30] as EH_2 before, which is a complex defect associated with more than one level as the peak is asymmetric. In the present work, it was supposed to be a combination of the Z_1/Z_2 center and other deeper level defects. Moreover, S2 is related to $RD_{1/2}$ or EH5, as the outcome of multiple irradiation. It can be inferred that ET1 (the Z_1/Z_2 center) and S1 (evolved from ET1) are the main reasons for affecting μ_n of the electron irradiated and multiple irradiated samples, respectively, since the conduction resistance showed a good relationship to their N_T.

3.3. TCAD simulations

As discussed above, the degradation of forward *I-V* characteristic after performing electron irradiation and multiple irradiation was mainly due to the decrease of the carrier mobility μ_n caused by the induced deep level defects. The μ_n in the drift region of the different irradiated-devices were quantitatively analyzed by conducting TCAD simulations. The schematic diagram of the SiC JBS is shown in Fig. 8, which was established based on the electrical test results of the DUTs and the TEM morphology characterization results. The tested and simulated results of the unirradiated and electron-irradiated samples are

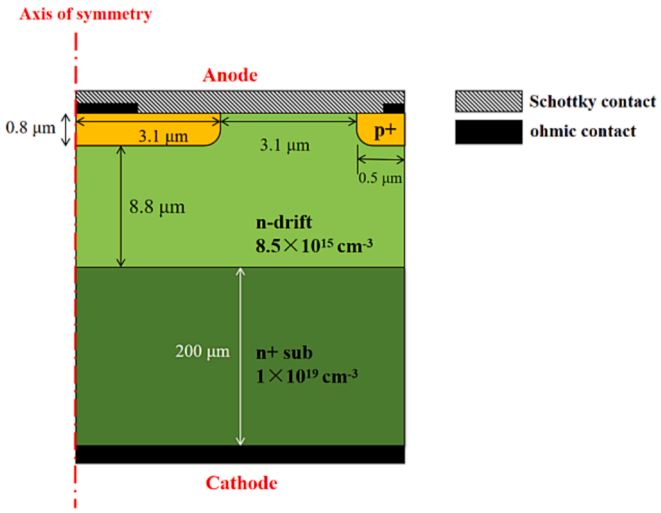

Fig. 8. Schematic diagram (hexagonal cell) of DUT in TCAD simulations.

illustrated in Fig. 9.

For the doped SiC, the impurity scattering and lattice scattering are dominant, compared to piezoelectric scattering, and the system default low-field electron mobility of 4H-SiC is 950 $cm^2/V{\cdot}s$ [31]. By adjusting the mobility, the fitted forward *I-V* curves after electron irradiation were obtained and shown in Fig. 9 (a), which had a good fit degree with the tested results. The fitted μ_n of samples after electron irradiation and multiple irradiation are listed in Table 5.

A further reduction in μ_n of the multiple irradiated samples based on simple electron irradiation can be observed. The relationship between the calculated mobility and the irradiation fluences is shown in Fig. 10. Particularly, in Fig. 10 (a), the mobility after simple electron irradiation exponentially decreased with the increase in the logarithm of the electron fluences. Furthermore, the relationship between the mobility of the samples after multiple irradiation and the HI fluences is shown in Fig. 10 (b). The relative fit curve and the fit equation are also displayed, indicating that every fit curve can be expressed as an exponential equation.

For simple electron irradiation, it can be seen that the mobility shows a significant decrease from the fluence of 1E13 e/cm^2. According to the current trends, the carrier mobility would decrease to zero when the fluences closely come to 1E17 e/cm^2. It has a similar trend with the experimental resultsin Ref. [32], where it has been reported that the epilayer mobility would have a sharp decrease first when the total deep level concentration exceeds 2E14 cm^{-3} (dose of 100 kGy) and finally decrease to zero when comes to 5E15 cm^{-3} (dose of 700 kGy). As far as

Table 5
The mobility simulated by TCAD after different irradiations.

Electron irradiated samples	unirradiated	1E14	1E15	1E16
μ_n ($cm^2/V{\cdot}s$)	950	925	870	670
1E15 groups[a]	**1E15**	**M1**	**M2**	**M3**
μ_n ($cm^2/V{\cdot}s$)	870	855	853	850
1E16 groups[a]	**1E16**	**M4**	**M5**	**M6**
μ_n ($cm^2/V{\cdot}s$)	670	640	630	610

[a] 1E15 groups mean all the samples that have received 1E15 e/cm^2 electron irradiation, including 1E15 e/cm^2 sample and M1 ~ M3. 1E16 groups includes 1E16 e/cm^2 sample and M4 ~ M6.

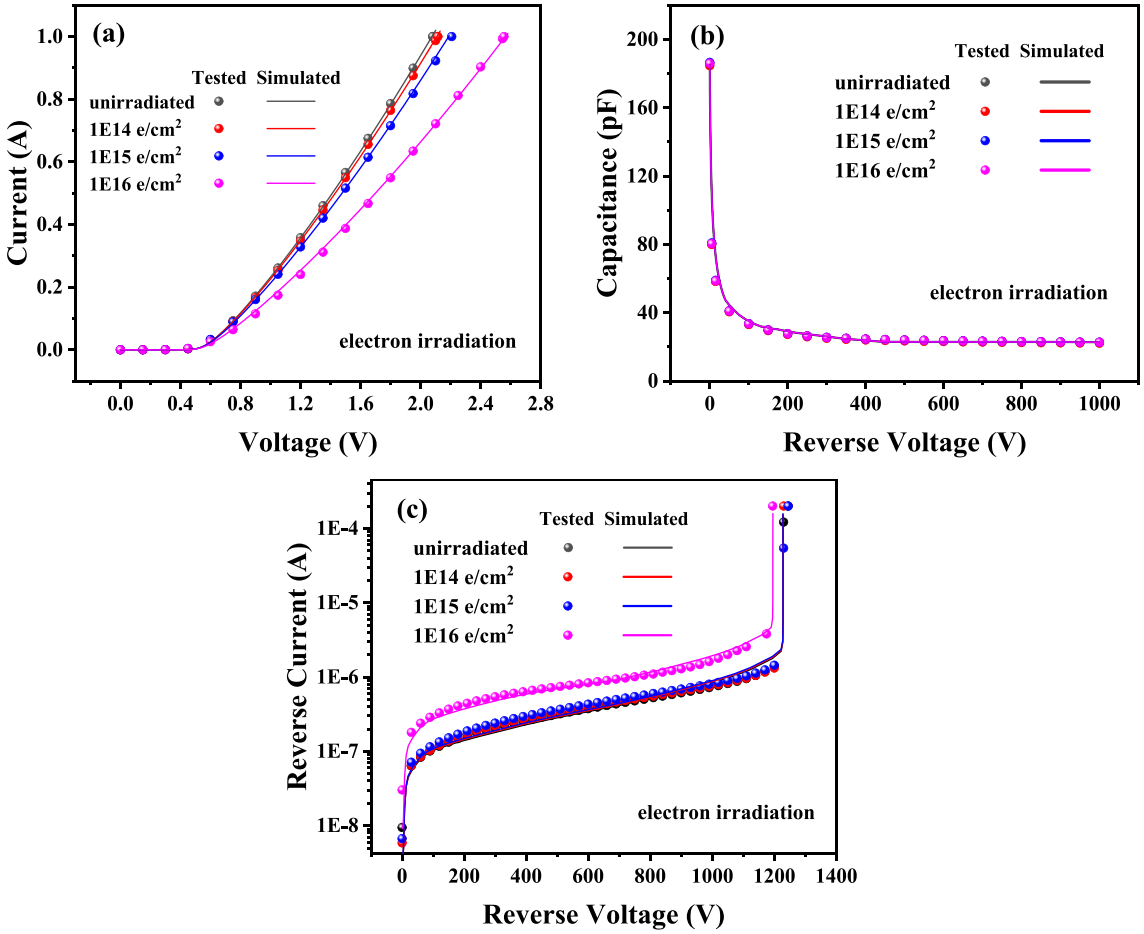

Fig. 9. The comparison between tested and simulated results of (a) forward *I-V*, (b) *C-V*, and (c) breakdown characteristics after electron irradiation.

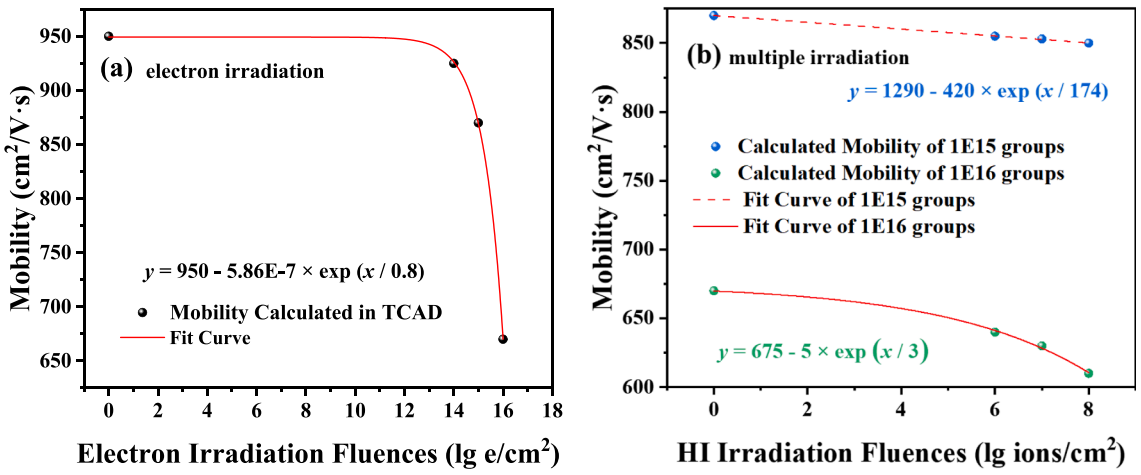

Fig. 10. The fit curve of the carrier mobility after (a) electron irradiation and (b) multiple irradiation calculated in TCAD simulation.

multiple irradiation are concerned, the degree of simulation depends on the fluence of both irradiation sources. When the electron fluence increased, the synergistic effects of HI irradiation became more obvious and the fit equation was closer to the exponential form. However, a more precise relationship should be built through more irradiation fluence conditions.

4. Conclusions

In this work, 1200 V commercial SiC JBSs were thoroughly studied at various irradiation conditions, namely heavy ion irradiation, electron irradiation, and multiple irradiation (HI + electron irradiation). It was for the first time discovered that the irradiation damages in SiC JBSs caused by two kinds of sources cannot be ascribed to a simple overlapping process. Diverse behaviors of the various irradiation conditions were also found in both the electrical characteristics and DLTS results. In addition, TCAD simulations were used to obtain the exact carrier mobility of samples. The main conclusions of the research are summarized below.

First, in terms of electrical characteristics, DUTs after simple HI irradiation did not show significant differences compared to the unirradiated sample. It was assumed that the degree of damage is limited by the total fluences of HI irradiation. After performing simple electron irradiation, the forward conduction characteristics experienced varying degrees of degradation, proportional to the fluences of the electron irradiation, while the *C-V* and breakdown characteristics remained unchanged, suggesting that the irradiation may cause a significant decrease in carrier mobility μ_n. After carrying out multiple irradiation, the damage of DUTs mainly depends on the fluence of electrons rather than HIs.

In addition, DLTS was used to analyze the deep level defects in the SiC JBSs. From the acquired results, it was shown that different sources of irradiation will induce several types of defects, which play different roles in the conductive properties. It was inferred that the ET1 (Z_1/Z_2 center) from simple electron irradiation and S1 (evolved from ET1) from multiple irradiation are the main reasons for affecting μ_n of the irradiated samples, respectively. Moreover, the μ_n in the drift region of the different irradiated devices were quantitatively analyzed by conducting TCAD simulations. Finally, the relationship between the mobility and the irradiation fluence was given. A more precise relationship should be developed in the future by taking into account more irradiation fluence conditions.

CRediT authorship contribution statement

Mu He: Conceptualization, Data curation, Formal analysis, Methodology, Writing – original draft, Writing – review & editing. **Xiaoping Dong:** Data curation, Methodology, Validation. **Meiju Xiang:** Data curation, Investigation, Visualization. **Yao Ma:** Conceptualization, Project administration, Supervision, Writing – review & editing. **Mingmin Huang:** Methodology, Project administration, Software, Writing – review & editing. **Sijie Zhang:** Data curation, Supervision. **Qingkui Yu:** Methodology, Resources. **Shuang Cao:** Investigation, Methodology. **Zhongyu Lu:** Data curation, Resources. **Yun Li:** Project administration. **Zhimei Yang:** Funding acquisition, Project administration. **Min Gong:** Project administration, Supervision.

Declaration of competing interest

The authors declare that they have no known competing financial interests or personal relationships that could have appeared to influence the work reported in this paper.

Data availability

No data was used for the research described in the article.

Acknowledgment

This project is supported by the Natural Science Foundation of Sichuan Province under Grant No. 2022NSFSC0874.

References

[1] J.L. Hudgins, Wide and narrow bandgap semiconductors for power electronics: a new valuation, Electron. Mater. 32 (6) (2003) 471–477.
[2] R. Singh, Reliability and performance limitations in SiC power devices, Microelectron. Reliab. 46 (5–6) (2006) 713–730.
[3] K. Car, C. Cos_kun, S. Aydoğan, et al., The effect of the electron irradiation on the series resistance of Au/Ni/6H-SiC and Au/Ni/4H-SiC Schottky contacts, Nucl. Instrum. Methods Phys. Res., B 268 (2010) 616–621.
[4] J. Garcia Lopez, M.C. Jimenez-Ramos, M. Rodriguez-Ramos, et al., Comparative study by IBIC of Si and SiC diodes irradiated with highenergy protons, Nucl. Instrum. Methods Phys. Res. B 372 (2016) 143–150.
[5] Z.M. Yang, Y. Li, Y. Ma, et al., XTEM investigation of recovery on electricaldegradation of 4H-SiC schottky barrier diode by swift heavy 209Bi ions irradiation, Nucl. Instrum. Methods Phys. Res., Sect. B 407 (2017) 304–309.
[6] J.L. Barth, Space, atmospheric, and terrestrial radiation environments, IEEE Transactions on Nuclear Science 50 (3) (2003) 466–482.
[7] E.R. Benton, Space radiation dosimetry in low-Earth orbit and beyond, Nuclear Instruments and Methods in Physics Research Section b: Beam Interactions with Materials and Atoms (2001).
[8] L.C. Simonsen, T.C. Slaba, P. Guida, et al., NASA's first ground-based galactic cosmic ray simulator: enabling a new era in space radiobiology research, PLOS Biology 18 (5) (2020) e3000669.
[9] A.L. Vampola, The hazardous space particle environment, IEEE Trans. Plasma Sci. 28 (6) (2000) 1831.

[10] S.K. Cheung, N.W. Cheung, Extraction of Schottky diode parameters from forward current-voltage characteristics[J], Appl. Phys. Lett. 49 (1986) 85–87.
[11] S.M. Sze, D.C. Mattis, Physics of semiconductor devices, Wiley, New York, 1981.
[12] A.F. Hamida, Z. Ouennoughi, A. Sellai, et al., Barrier inhomogeneities of tungstenschottky diodes on 4H-SiC, Semicond. Sci. Technol. 23 (4) (2008) 045005.
[13] H. Li, C. Liu, Y. Zhang, et al., Irradiation effect of primary knock-on atoms on conductivity compensation in N-type 4H-SiC Schottky diode under various irradiations, Semiconductor Science and Technology 34 (9) (2019), 095010.1-095010.8.
[14] V.V. Kozlovski, A.A. Lebedev, E.V. Bogdanova, Model for conductivity compensation of moderately doped n- and p-4H-SiC by high-energy electron bombardment, Journal of Applied Physics 117 (15) (2015) 155702.
[15] P. Hazdra, J. Vobeck, Radiation defects created in n-type 4H-SiC by electron irradiation in the energy range of 1–10MeV, Physica Status Solidi (a) 216 (17) (2019).
[16] V.V. Kozlovski, V.V. Emtsev, A.M. Ivanov, et al., Charge carrier removal rates in n-type silicon and silicon carbide subjected to electron and proton irradiation, Physica. b, Condensed Matter 404 (23–24) (2009) 4752–4754.
[17] M.J. Xiang, D.W. Wang, M. He, et al., Electrical characterization and temperature reliability of 4H-SiC schottky barrier diodes after electron radiation, Microelectronics and Reliability 141 (2023) 114886.
[18] P. Hazdra, J. Vobeck, Radiation defects created in n-type 4H-SiC by electron irradiation in the energy range of 1–10 MeV, Physica Status Solidi (a) 216 (17) (2019).
[19] E. Omotoso, A.T. Paradzah, P.J. Rensburg, et al., Electrical characterisation of deep level defects created by bombarding the n-type 4H-SiC with 1.8 MeV protons, Surface & Coatings Technology 355 (2018).
[20] E.K. Liu, B.S. Zhu, J.S. Luo, The Physics of Semiconductors, (7th Edition)., Publishing House of Electronics Industry, 2017 in Chinese.
[21] D.V. Lang, Deep-level transient spectroscopy: a new method to characterize traps in semiconductors, Journal of Applied Physics (1974).
[22] L. Storasta, J.P. Bergman, E. Janzén, et al., Deep levels created by low energy electron irradiation in 4H-SiC, Journal of Applied Physics (2004).
[23] R.P. Vigneshwara, N.V.L. Narasimha Murty, Thermally stimulated capacitance in gamma irradiated epitaxial 4H-SiC Schottky barrier diodes, Journal of Applied Physics 123 (16) (2018) 161536.
[24] I. Iskandarova, Khromov, et al., The role of neutral point defects in carrier mobility degradation in bulk 4H-SiC and at 4H-SiC/SiO2 interface: First-principles investigation using Green's functions, Journal of Applied Physics (2015).
[25] E. Omotoso, W.E. Meyer, E. Igumbor, et al., DLTS study of the influence of annealing on deep level defects induced in xenon ions implanted n-type 4H-SiC, Journal of Materials Science: Materials in Electronics 33 (19) (2022) 15679–15688.
[26] D.S. Chao, H.Y. Shih, J.Y. Jiang, et al., Influence of displacement damage induced by neutron irradiation on effective carrier density in 4H-SiC JBSs and MOSFETs, Japanese Journal of Applied Physics 58 (SB) (2019) SBBD08.
[27] P. Carlsson, N.T. Son, F.C. Beyer, et al., Deep levels in low-energy electron-irradiated 4H-SiC, Physica Status Solidi (RRL) -Rapid Research Letters 3 (4) (2009).
[28] J. Zhang, L. Storasta, J.P. Bergman, et al., Electrically active defects in n-type 4H-silicon carbide grown in a vertical hot-wall reactor, Journal of Applied Physics 93 (8) (2003) 4708–4714.
[29] T. Dalibor, G. Pensl, H. Matsunami, et al., Deep defect centers in silicon carbide monitored with deep level transient spectroscopy, Physica Status Solidi (a) 162 (1) (1997) 199–225.
[30] Z.M. Yang, F. Lan, Y. Li, et al., The effect of the interfacial states by swift heavy ion induced atomic migration in 4H-SiC Schottky barrier diodes, Nuclear Instruments and Methods in Physics Research Section b: Beam Interactions with Materials and Atoms 436 (2018) 244–248.
[31] T. Ayalew, SiC Semiconductor Devices, Technology, Modeling, and Simulation, Technishen Universiaet Wien, Austria, 2004.
[32] J. Vobecky, P. Hazdra, S. Popelka, et al., Impact of Electron Irradiation on the ON-State Characteristics of a 4H–SiC JBS Diode, Electron Devices IEEE Transactions on 62 (6) (2015) 1964–1969.